

Crossover Equation of State for the Thermodynamic Properties of Mixtures of Methane and Ethane in the Critical Region

A. A. Povodyrev,^{1,2} G. X. Jin,^{1,3} S. B. Kiselev,² and J. V. Sengers^{1,4,5}

Received October 4, 1995

We present an equation of state for the thermodynamic properties of mixtures of methane and ethane in the critical region that incorporates the crossover from singular thermodynamic behavior near the locus of vapor-liquid critical points to regular thermodynamic behavior outside the critical region. The equation of state yields a satisfactory representation of the thermodynamic-property data for the mixtures in a large range of temperatures and densities.

KEY WORDS: critical phenomena; equation of state; ethane; methane; plait point; thermodynamic properties.

1. INTRODUCTION

Asymptotically close to the critical point the thermodynamic properties of fluids satisfy scaling laws with universal scaling functions that are the same as those for the three-dimensional Ising model [1-3]. Binary mixtures belong to the same universality class and have the same expressions for the thermodynamic properties provided that suitable isomorphic variables are used [4-6]. To extend the description of the properties to a wider region around the critical point one needs to incorporate crossover from Ising-like

¹ Institute for Physical Science and Technology, University of Maryland, College Park, Maryland 20742, U.S.A.

² Department of Physics, Institute for Oil and Gas Research of the Russian Academy of Sciences, Leninskii Prospekt 65/2, Moscow 117917, Russia.

³ Present address: Laboratory of Neuropsychology, National Institute of Health, Bethesda, Maryland 20892, U.S.A.

⁴ Department of Chemical Engineering, University of Maryland, College Park, Maryland 20742, U.S.A.

⁵ To whom correspondence should be addressed.

asymptotic behavior near the critical point to mean-field (van der Waals-like) behavior far away from the critical point. Such a crossover equation of state has been developed by Chen et al. for one-component fluids [7] and extended to mixtures by Jin et al. [8]. In this paper we adopt an improved version of the crossover equation of state proposed by Jin [9] and apply it to mixtures of methane and ethane.

2. ISOMORPHIC FREE-ENERGY DENSITY

The theory of critical phenomena in one-component fluids can be extended to mixtures provided that one uses appropriate isomorphic thermodynamic quantities [4–6, 10]. For this purpose we use here the thermodynamic variables adopted by Jin et al. [8] as further discussed by Anisimov and Sengers [11].

Let U , A , and V be the specific internal energy, Helmholtz free energy and volume taken per mole. For one-component fluids the critical crossover behavior of the thermodynamic properties has been specified in terms of the Helmholtz free-energy density A/V as a function of the density $\rho = 1/V$ and the inverse temperature $1/T$ [7, 12–14]. To extend the theory to binary mixtures, we define [8, 11]

$$\hat{T} = \frac{1}{RT}, \quad \hat{P} = \frac{P}{RT}, \quad \hat{\mu}_1 = \frac{\mu_1}{RT}, \quad \hat{\mu}_2 = \frac{\mu_2}{RT}, \quad \hat{A} = \frac{\rho A}{RT} \quad (1)$$

where P is the pressure, μ_1 and μ_2 are the chemical potentials of the two components, and R is the molar gas constant.

The extension of the theory to mixtures is based on the principle that a suitably chosen isomorphic free-energy density will have the same form as the Helmholtz free-energy density of one-component fluids. One possibility is to treat the chemical potential μ_1 of one of the components referred to as the solvent as the ordering field and the chemical-potential difference $\mu = \mu_2 - \mu_1$ as a hidden or irrelevant field. A dimensionless isomorphic free-energy density \hat{A}_{iso} may then be defined as

$$\hat{A}_{\text{iso}} = \hat{A} - \rho \hat{\mu} x \quad (2)$$

so that

$$d\hat{A}_{\text{iso}} = \hat{u} d\hat{T} + \hat{\mu}_1 d\rho - x\rho d\hat{\mu} \quad (3)$$

where $\hat{\mu} = U/V$ is the energy density, x the mole fraction of the solute, and

$$\hat{\mu} = \hat{\mu}_2 - \hat{\mu}_1 \quad (4)$$

The choice of $\hat{\mu}_1$ as the ordering field and $\hat{\mu}$ as the hidden field is not convenient in practice, since in the pure-component limits $\hat{\mu}_1$ or $\hat{\mu}_2$ diverges. This problem was avoided by Leung and Griffiths [15], who introduced an ordering field h and a hidden field ζ that are related to the "activities" $e^{\hat{\mu}_1}$, and $e^{\hat{\mu}_2}$. In the form adopted by Jin et al. [8], they are defined by

$$h = \ln(e^{\hat{\mu}_1} + e^{\hat{\mu}_2}), \quad \zeta = \frac{1}{1 + e^{(\hat{\mu}_1 - \hat{\mu}_2)}} \quad (5)$$

so that

$$\hat{\mu}_1 = h + \ln(1 - \zeta), \quad \hat{\mu}_2 = h + \ln \zeta \quad (6)$$

A Legendre transformation of the form

$$\hat{A}_{\text{eff}} = h\rho - \hat{P} \quad (7)$$

yields

$$d\hat{A}_{\text{eff}} = \hat{u} d\hat{T} + h d\rho - w d\zeta \quad (8)$$

with

$$w = \frac{x - \zeta}{\zeta(1 - \zeta)} \rho \quad (9)$$

\hat{A}_{eff} and \hat{A}_{iso} are related by

$$\hat{A}_{\text{eff}} = \hat{A}_{\text{iso}} - \rho \ln(1 - \zeta) \quad (10)$$

\hat{A}_{eff} is an alternative dimensionless isomorphic free-energy density when taken at constant ζ . The advantage of the choice of \hat{A}_{eff} as the isomorphic free-energy density is that the hidden field variable ζ will vary from 0 to 1, when the concentration x varies from 0 to 1. Unlike the concentration x , the variable ζ will have the same value in two coexisting phases.

The present formulation of an equation of state for fluid mixtures in the critical region is restricted to fluid mixtures for which the critical points of the two pure components are connected by a continuous line of vapor-liquid critical points. The critical parameters T_c , ρ_c , and P_c will vary along this line of critical points as functions of the concentration x or, alternatively, as functions of the variable ζ . We find it convenient to introduce the deviation variables

$$\tau = \frac{T - T_c(\zeta)}{T}, \quad \Delta\tilde{p} = \frac{\rho - \rho_c(\zeta)}{\rho_c(\zeta)} \quad (11)$$

Equation (8) may then be rewritten as

$$d\hat{A}_{\text{eff}} = -\hat{U} d\tau + h d\rho - W d\zeta \tag{12}$$

with

$$\hat{U} = \hat{u}/RT_c(\zeta), \quad W = \frac{x - \zeta}{\zeta(1 - \zeta)} \rho + \hat{U} \frac{1}{T} \frac{dT_c}{d\zeta} \tag{13}$$

At fixed ζ , $\hat{A}_{\text{eff}}(\tau, \rho, \zeta)$ will be the same singular function of τ and ρ as the Helmholtz free-energy density of a one-component fluid [7], with all system-dependent constants depending parametrically on the hidden field ζ [8]. From Eqs. (12) and (13) it follows that the composition x is related to the variable ζ by

$$x = \zeta - \frac{\zeta(1 - \zeta)}{\rho} \left\{ \left[\frac{\partial \hat{A}_{\text{eff}}}{\partial \zeta} \right]_{\tau, \rho} - \frac{1}{T} \frac{dT_c(\zeta)}{d\zeta} \left[\frac{\partial \hat{A}_{\text{eff}}}{\partial \tau} \right]_{\zeta, \rho} \right\} \tag{14}$$

3. CROSSOVER FREE-ENERGY DENSITY

A crossover equation of state for the critical part $\Delta\tilde{A}$ of a dimensionless free-energy density $\tilde{A} = AT_c/VP_cT$ has been developed by Chen et al. for one-component fluids [7] and extended to mixtures by Jin et al. [8]. They start from a classical Landau expansion for $\Delta\tilde{A}$, which is then transformed or “renormalized” so as to incorporate the effects from long-range critical fluctuations. Retaining six terms in the classical Landau expansion they obtain for the renormalized free-energy density

$$\begin{aligned} \Delta\tilde{A}_r(t, M, \zeta) = & \frac{1}{2} t M^2 \mathcal{F} \mathcal{G} + \frac{1}{4!} u^* \bar{u}(\zeta) A(\zeta) M^4 \mathcal{G}^2 \mathcal{H} + \frac{1}{5!} a_{05}(\zeta) M^5 \mathcal{G}^{5/2} \mathcal{V} \mathcal{H} \\ & + \frac{1}{6!} a_{06}(\zeta) M^6 \mathcal{G}^3 \mathcal{H}^{3/2} + \frac{1}{4!} a_{14}(\zeta) t M^4 \mathcal{F} \mathcal{G}^2 \mathcal{H}^{1/2} \\ & + \frac{1}{2!2!} a_{22}(\zeta) t^2 M^2 \mathcal{F}^2 \mathcal{G} \mathcal{H}^{-1/2} - \frac{1}{2} t^2 \mathcal{K} \end{aligned} \tag{15}$$

where t is a temperature-like variable and M is a density-like variable that are related to the physical variables τ and $\Delta\tilde{p}$ by

$$t = c_r(\zeta)\tau + c(\zeta) \left[\frac{\partial \Delta\tilde{A}_r}{\partial M} \right]_{t, \zeta}, \quad M = c_p(\zeta)(\Delta\tilde{p} - d_1(\zeta)\tau) + c(\zeta) \left[\frac{\partial \Delta\tilde{A}_r}{\partial t} \right]_{M, \zeta} \tag{16}$$

Table I. Universal Constants

$\nu = 0.630$
$\eta = 0.0333$
$\alpha = 2 - 3\nu = 0.110$
$\omega = \Delta/\nu = 0.80952$
$\omega_a = 2.1$
$u^* = 0.472$

The coefficients $\bar{u}(\zeta)$, and $a_{ij}(\zeta)$ in Eq. (15) and $c_r(\zeta)$, $c_\rho(\zeta)$, $c(\zeta)$, and $d_1(\zeta)$ in Eq. (16) are system-dependent coefficients which, for mixtures, will depend on the variable ζ , while the coefficient u^* in Eq. (15) is a universal constant ($u^* = 0.472$). The functions \mathcal{F} , \mathcal{G} , \mathcal{H} , \mathcal{V} , and \mathcal{K} in Eq. (15) are rescaling functions that can be expressed in terms of a crossover function Y through

$$\begin{aligned} \mathcal{F} &= Y^{(2-1/\nu)/\omega}, & \mathcal{G} &= Y^{-\eta/\omega}, & \mathcal{H} &= Y^{1/\omega} \\ \mathcal{V} &= Y^{(\omega_a-1/2)/\omega}, & \mathcal{K} &= \frac{\nu}{\alpha\bar{u}\Delta} (Y^{-\alpha/\omega\nu} - 1) \end{aligned} \tag{17}$$

where ν , η , and $\alpha = 2 - 3\nu$ are universal critical exponents that characterize the asymptotic critical scaling behavior, while $\omega = \Delta/\nu$ ($\Delta = 0.51$) and $\omega_a = \Delta_a/\nu = 2.1$ are universal critical exponents associated with the leading symmetric and asymmetric correction terms [2, 16, 17]. The values of these universal constants are summarized in Table I.

The crossover function Y in the expressions, Eq. (17), for the rescaling functions is to be determined from the set of coupled algebraic equations

$$1 - [1 - \bar{u}(\zeta)] Y = \bar{u}(\zeta) \left[1 + \left(\frac{\Lambda(\zeta)}{\kappa} \right)^{\omega_c} \right]^{1/\omega_c} Y^{1/\omega} \tag{18}$$

$$\begin{aligned} \kappa^2 &= t\mathcal{F} + \frac{1}{2} M^2 \bar{u}(\zeta) u^* \Lambda \mathcal{G} \mathcal{H} + \frac{a_{05}(\zeta)}{6} M^3 \mathcal{G}^{3/2} \mathcal{V} \mathcal{H} \\ &+ \frac{a_{06}(\zeta)}{24} M^4 \mathcal{G}^2 \mathcal{H}^{3/2} \\ &+ \frac{a_{14}(\zeta)}{2} t M^2 \mathcal{F} \mathcal{G} \mathcal{H}^{1/2} + \frac{a_{22}(\zeta)}{2} t^2 \mathcal{F}^2 \mathcal{H}^{-1/2} \end{aligned} \tag{19}$$

Equations (18) and (19) are those recently proposed by Jin et al. [9, 18]. They differ from those employed earlier by our research group [7, 8, 12] in two respects, namely, in the choice of the exponent ω_c in Eq. (18) and in the number of terms retained in Eq. (19) for κ^2 . While in the earlier work the renormalized expansion Eq. (15) for $\Delta\tilde{A}_r$, based on a six-term Landau expansion was introduced, only the first two terms in the corresponding expansion, Eq. (19), for κ^2 were retained. Equation (19) is more fully consistent with the number of terms retained in the Landau expansion for the free-energy density. The parameter κ is closely related to the inverse correlation length [19] and serves as a measure of the distance from the critical point [20]. In the asymptotic critical limit

$$\lim_{A/\kappa \rightarrow \infty} Y = \left(\frac{\kappa}{\tilde{\mu}A}\right)^\omega \tag{20}$$

and one recovers from Eq. (15) the asymptotic critical power laws with leading Wegner correction terms [21]. The classical limit corresponds to

$$\lim_{A/\kappa \rightarrow 0} Y = 1 \tag{21}$$

so that Eq. (15) reduces to the classical Landau expansion.

The exponent ω_c in Eq. (18) is an exponent that accounts for the rate at which the final crossover to the classical limit occurs. The higher the value of ω_c , the faster we reach the classical limit, i.e., the faster Y will go to unity when we move away from the critical point. From an analysis of the spherical model, Nicoll and Bhattacharjee [22] found $\omega_c = 2$, and this is the value that has been adopted in our previous work [7, 8, 12, 19]. However, higher-order terms in the Landau expansion may contribute to the actual crossover behavior and we found that an effective value 3/2 for the exponent ω_c yielded empirically an increased range of validity of the crossover equation of state [9, 14].

The actual dimensionless free energy density $\Delta\tilde{A}$ is related to $\Delta\tilde{A}_r$, given by Eq. (15), by a transformation of the form [7, 8]

$$\Delta\tilde{A}(\tau, \Delta\tilde{p}, \zeta) = \Delta\tilde{A}_r(t, M, \zeta) - c(\zeta) \left[\frac{\partial \Delta\tilde{A}_r}{\partial M} \right]_{t, \zeta} \left[\frac{\partial \Delta\tilde{A}_r}{\partial t} \right]_{M, \zeta} \tag{22}$$

Taking into account the different ways in which \hat{A} and \tilde{A} have been made dimensionless, we obtain for the effective Helmholtz free-energy density

$$\hat{A}_{\text{eff}}(\tau, \rho, \zeta) = \frac{P_c(\zeta)}{RT_c(\zeta)} [\Delta\tilde{A}(\tau, \Delta\tilde{p}, \zeta) + \tilde{A}_0(\tau, \zeta) + \rho h_0(\tau, \zeta)] \tag{23}$$

where $\tilde{A}_0(\tau, \zeta)$ and $h_0(\tau, \zeta)$ represent analytic noncritical contributions, which in practice are represented by truncated Taylor series expansions:

$$\tilde{A}_0(\tau, \zeta) = \sum_{j=0}^4 \tilde{A}_j(\zeta) \tau^j, \quad h_0(\tau, \zeta) = \frac{1}{\rho_c(\zeta)} \sum_{j=0}^7 \tilde{\mu}_j(\zeta) \tau^j \quad (24)$$

with system-dependent coefficients $\tilde{A}_j(\zeta)$ and $\tilde{\mu}_j(\zeta)$. Since $\hat{A} - \rho(\partial\hat{A}/\partial\rho)_\tau = -\hat{P}$, it follows that $\tilde{A}_0(\zeta) \equiv -1$.

Equation (23) yields a fundamental equation for the effective Helmholtz free-energy density from which all other thermodynamic properties can be calculated. Some of the relevant thermodynamic derivatives are given in Appendix A. In this paper we apply the equation of state, given by Eq. (23), first to methane and to ethane and then to mixtures of methane (component 1) and ethane (component 2).

4. APPLICATION TO ONE-COMPONENT FLUIDS

The crossover equation of state for the one-component fluids are obtained from Eq. (23) by taking $\zeta=0$ (methane) and $\zeta=1$ (ethane). To specify the crossover equation of state we need the critical parameters $T_c^{(i)}$, $\rho_c^{(i)}$, and $P_c^{(i)}$, where superscript $i=1$ corresponds to methane and $i=2$ to ethane. The values of the critical parameters are either obtained from direct experimental observations or deduced from an asymptotic analysis of experimental thermodynamic data very close to the critical point.

The crossover parameters $\bar{u}^{(i)}$ and $A^{(i)}$, the scaling field parameters $c_r^{(i)}$, $c_\rho^{(i)}$, $c^{(i)}$ and $d_1^{(i)}$, the coefficients $a_{jk}^{(i)}$ of the Landau expansion, and the background parameters $\tilde{A}_j^{(i)}$ are to be determined from a fit of the crossover equation of state to experimental P - ρ - T data for methane and ethane. The coefficients $\tilde{\mu}_j^{(i)}$ for $j \geq 2$ determine background contributions to the caloric properties and can be obtained from fits to experimental specific heat capacities or speed-of-sound data. The coefficients $\tilde{\mu}_0^{(i)}$ and $\tilde{\mu}_1^{(i)}$ are related to the zero points of entropy and energy of the two fluid components and they do not enter into the calculation of experimentally observable thermodynamic properties like pressures and specific heat capacities. However, for the mixtures $\tilde{\mu}_0(\zeta)$ and $\tilde{\mu}_1(\zeta)$ are no longer arbitrary, since they are related to the entropy of mixing and energy of mixing as further discussed in Section 5.

Scientists at the National Institute of Standards and Technology have developed a computer program for the calculation of the thermodynamic properties of mixtures, including mixtures of methane and ethane [23], referred to as NIST14 [24, 25]. This computer program is based on a classical principle of extended corresponding states and, hence, does not

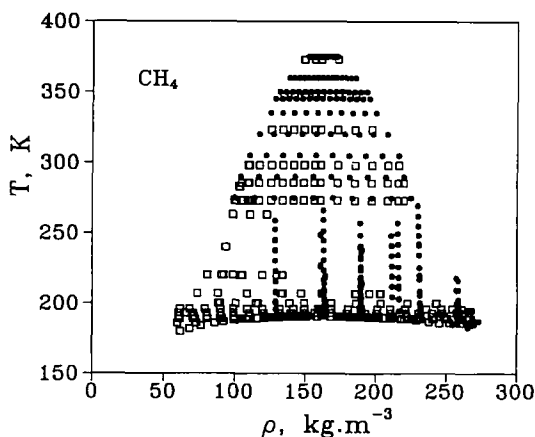


Fig. 1. Range of validity of the crossover equation of state for methane. (□) Experimental P - ρ - T data [29–31]; (●) Experimental C_r data [32–34] and C_r values calculated from the global equation [27].

attempt to include the singular behavior of the thermodynamic properties of fluids near the critical point. However, NIST14 does yield a satisfactory representation of the thermodynamic properties of mixtures of methane and ethane away from the critical locus of the mixture. We have, therefore, made an attempt to make our crossover equation of state consistent with the values calculated from NIST14 outside the critical region.

4.1. Methane

Jin et al. [26] have applied an earlier simpler version of our crossover equation of state to methane to be used in conjunction with a global equation of state developed for methane by Setzmann and Wagner [27]. However, in order to develop a theoretically based equation of state for mixtures in the critical region, we want to start from a single crossover equation of state for the two pure-fluid components applicable in as large a range of temperatures and densities as possible. Hence we rerepresent the thermodynamic properties of methane in terms of the crossover equation of state formulated in this paper. For the critical parameters of methane we continued to use the values obtained by Kleinrahm and Wagner [28] and adopted by Setzmann and Wagner [27] and by Jin et al. [26]

$$T_c^{(1)} = 190.564 \text{ K}, \quad P_c^{(1)} = 4.5992 \text{ MPa}, \quad \rho_c^{(1)} = 10.122 \text{ mol} \cdot \text{L}^{-1} \quad (25)$$

The system-dependent coefficients, except for $\tilde{\mu}_j^{(1)}$, were determined by fitting the crossover equation of state to experimental P - ρ - T data reported by Wagner and co-workers [29, 30] and by Trappeniers et al. [31]. With estimated errors in pressure, temperature and density as small $\sigma_p = 5 \times 10^{-5}$ MPa, $\sigma_T = 1 \times 10^{-3}$ K, and $\sigma_\rho = 0.15$ kg.m $^{-3}$ [26], we find that the equation represents the experimental data with a reduced chi-square of 3.57 in a range of temperatures and densities bounded by

$$\tau + 1.2\Delta\bar{\rho}^2 < 0.5, \quad \tau > -0.07 \quad (26)$$

This range of temperatures and densities is shown in Fig. 1. Percentage deviations of the experimental pressures from the calculated pressures are shown in Fig. 2; they are generally within 0.15% inside the region specified above except near the boundary at higher densities, where the deviations increase up to 0.35%.

The coefficients $\mu_j^{(1)}$ ($j \geq 3$) account for background contributions to the caloric properties and they were determined by fitting the crossover equation to experimental specific heat capacities and speed-of-sound data. Specifically, we used experimental C_V data obtained by Younglove [32] as corrected by Roder [33], experimental C_V data obtained by Anisimov et al. [34] with temperatures shifted by 0.114 K as discussed by Kiselev and Sengers [35], and experimental speed-of-sound data obtained by Gammon and Douslin [36], by Straty [37], and by Trusler and Zazari [38]. In addition we used C_V values calculated from the global equation [27] at

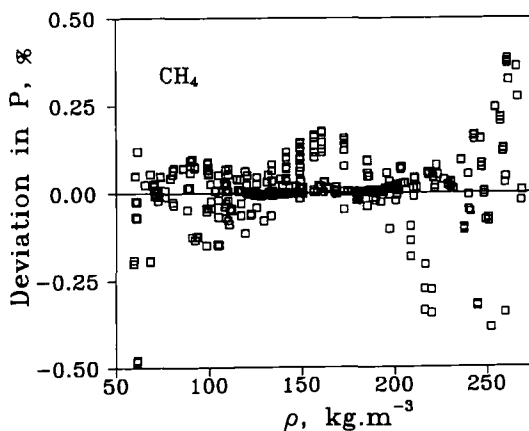


Fig. 2. Percentage deviations of the experimental pressures reported by Wagner and co-workers [29, 30] and by Trappeniers and co-workers [31] for methane from values calculated with the crossover equation of state.

temperatures up to 375 K in the far away region. The C_V data are represented with a standard deviation of 2.5% and the speed-of-sound data with a standard deviation of 1.5%, which is within the accuracy of the experimental data. The values of the system-dependent coefficients in our crossover equation of state are presented in Table II. Percentage deviations of the experimental C_V data from the calculated values of C_V are shown in Fig. 3. The coefficient $\tilde{\mu}_1^{(1)}$ was arbitrarily set to zero.

The actual values for the speed of sound of methane are shown in Fig. 4. Figure 4 confirms that our crossover equation of state yields a good representation of the speed of sound in a large range of temperatures. In Fig. 5 we show a comparison of our crossover equation with experimental

Table II. System-Dependent Constants

Parameter	$k^{(1)}$ (methane)	$k^{(2)}$ (ethane)	$k^{(m)}$
Crossover			
\tilde{u}	0.3550	0.3695	0
A	0.8793	1.0000	0
Scaling-field			
c_1	1.2827	1.5233	-0.763
c_ρ	2.5899	2.4897	0.417
c	-0.0940	-0.09919	0
d_1	-0.7586	-0.8601	0
Classical			
a_{05}	0.1873	0.2565	0
a_{06}	0.5337	0.7511	0
a_{14}	0.3752	0.3648	0
a_{22}	1.1540	1.187	0
Equation-of-state background			
\tilde{A}_1	-4.9787	-5.4366	9.088
\tilde{A}_2	5.9455	7.0270	24.227
\tilde{A}_3	3.3181	6.9056	0.713
\tilde{A}_4	-5.214	-11.758	0
Caloric background			
$\tilde{\mu}_1$	0	-2.16	1.747
$\tilde{\mu}_2$	-12.924	-19.23	3.11
$\tilde{\mu}_3$	-9.0926	-18.59	34.358
$\tilde{\mu}_4$	6.3061	10.45	-26.523
$\tilde{\mu}_5$	-14.218	-33.58	89.72
$\tilde{\mu}_6$	0	0	42.457
$\tilde{\mu}_7$	0	0	-186.4
Molar mass (g · mol ⁻¹)	16.043	30.069	

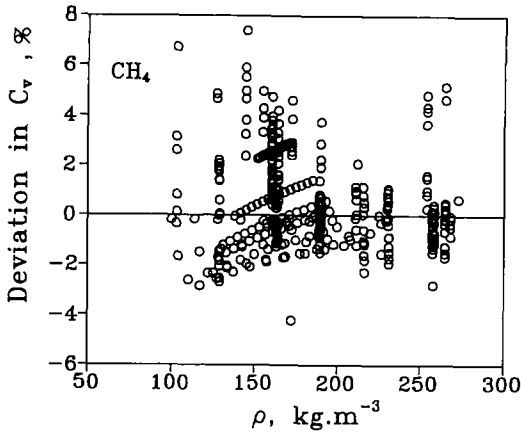


Fig. 3. Percentage deviations of the experimental C_p data [32-34] for methane from values calculated with the crossover equation of state.

C_p data reported by Kasteren and Zeldenrust [39] and by Jones et al. [40], which were not used in the determination of the values of the system-dependent constants for methane.

In Fig. 6 we show the densities and saturation pressures of the coexisting vapor and liquid phases below the critical temperature compared with the experimental data reported by Kleinrahm and Wagner [28], which

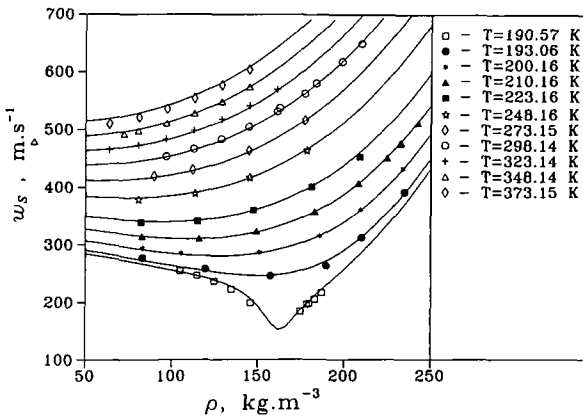


Fig. 4. Sound velocity of ethane at various temperatures as a function of density. The symbols indicate experimental data [36-38] and the curves represent values calculated with the crossover model.

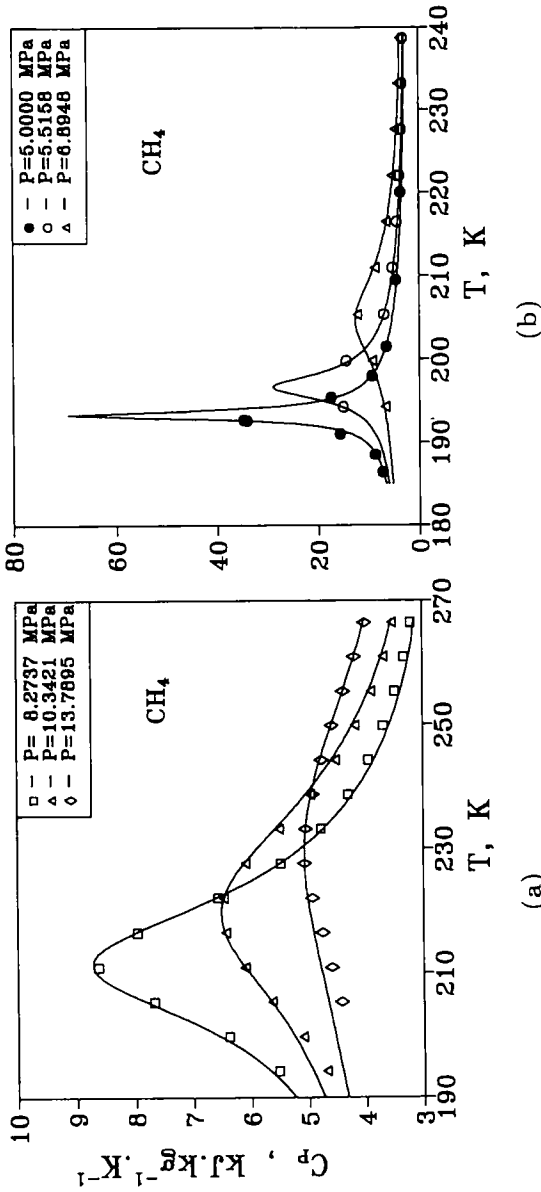


Fig. 5. The isobaric specific heat capacity C_p of methane at various pressures as a function of temperature. The filled symbols indicate experimental data obtained by Kasteren and Zeldenrust [39], the open symbols experimental data obtained by Jones et al. [40], and the curves values calculated with the crossover equation of state.

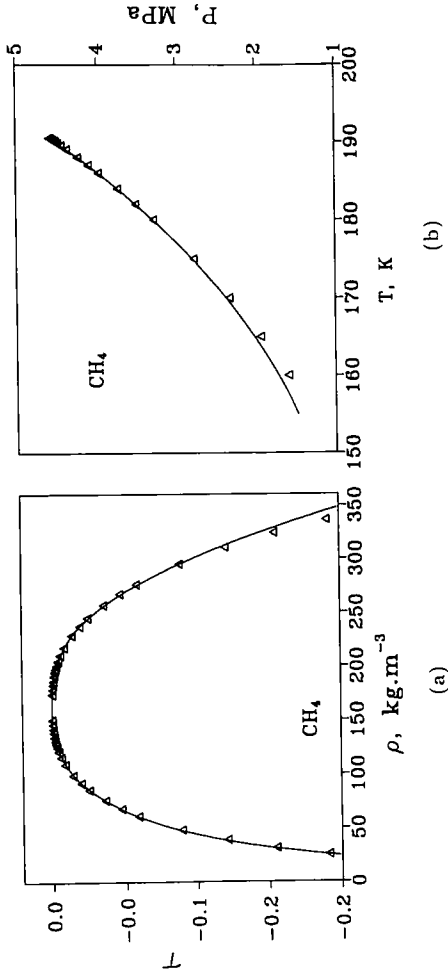


Fig. 6. Densities (a) and saturation pressures (b) of the coexisting vapor and liquid phases of methane below the critical temperature. The symbols represent experimental data reported by Kleinrahm and Wagner [28] and the curves represent the values calculated with the crossover equation of state.

were not used in the fits of the crossover equation. The figure confirms that below the critical temperature, the crossover equation yields a satisfactory representation of the data for $T \leq 175$ K, i.e., for $\tau > -0.07$ as specified in Eq. (26). Below 175 K there are some systematic deviations for the vapor pressures and liquid densities.

An alternative, more phenomenological crossover equation of state for methane and ethane has been proposed by Kiselev and Sengers [35]. This alternative crossover equation of state is discussed in Appendix B and its range of validity is comparable to the range of validity, Eq. (26), of the crossover equation formulated in the present paper. The crossover equation of Kiselev and Sengers and our crossover equation represent the experimental P - ρ - T data with similar accuracy. Our crossover equation yields a good representation of the isochoric specific heat calculated from the global equation of Setzmann and Wagner [27] at temperatures farther away from T_c up to $T = 375$ K, but the crossover equation of Kiselev and Sengers is in better agreement with experimental C_V data of Anisimov et al. [34] very close to T_c . In Fig. 7 we have plotted C_P and C_V of methane as a function of temperature at $\rho = \rho_c$ as calculated from the crossover equation presented in this paper, from the earlier crossover equation of Jin et al. [26] and from the crossover equation of Kiselev and Sengers [35]. Our crossover equation and the earlier crossover equation of Jin et al. [26] yield essentially identical results. The difference between the values of the specific heat capacities as calculated from our crossover equation and that of Kiselev and Sengers [35] is probably a measure of the absolute accuracy with which the specific heat capacities of methane near the critical point can be calculated.

4.2. Ethane

The crossover equation of state described in this paper was originally formulated by Jin and applied to ethane [9, 18]. The values adopted for the critical parameters of ethane are [18]

$$T_c^{(2)} = 305.322 \text{ K}, \quad P_c = 4.8718 \text{ MPa}, \quad \rho_c^{(2)} = 6.8592 \text{ mol} \cdot \text{L}^{-1} \quad (27)$$

The values of $\tilde{u}^{(2)}$, $A^{(2)}$, $c_t^{(2)}$, $c_\rho^{(2)}$, $c^{(2)}$, $d_1^{(2)}$, $a_{jk}^{(2)}$, and $\tilde{A}_j^{(2)}$ were obtained by fitting the crossover equation of state to experimental P - ρ - T data reported by Douslin and Harrison [41]. The values of $\tilde{\mu}_j^{(2)}$ were determined from a fit to experimental C_V data reported by Shmakov [42]. A comparison of the crossover equation with the experimental P - ρ - T and C_V data for ethane will be presented elsewhere [18]. Here we show in Fig. 8 only the densities and saturation pressures of the coexisting vapor and liquid phases below the critical temperature. This figure is to be compared with Fig. 6 for methane.

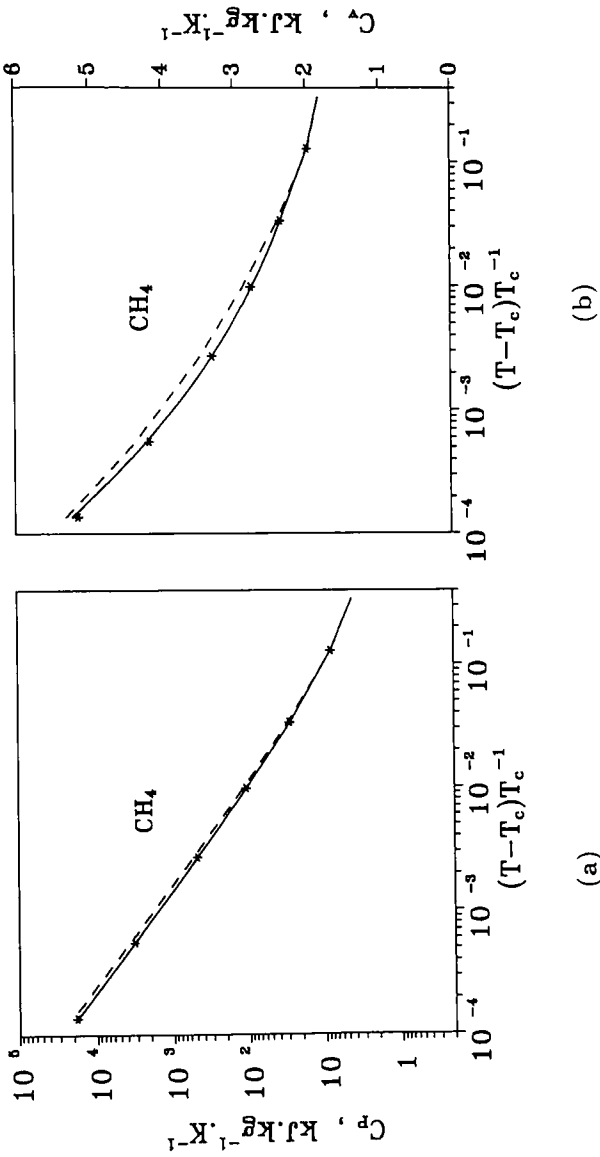


Fig. 7. Isobaric specific heat capacity C_p (a) and the isochoric specific heat capacity C_v (b) of methane at the critical density as a function of temperature. The solid curve represents values calculated with the crossover equation presented in this paper, the asterisks values calculated with the earlier crossover equation of Jin et al. [26], and the dashed curves values calculated with the crossover equation of Kiselev and Sengers [35].

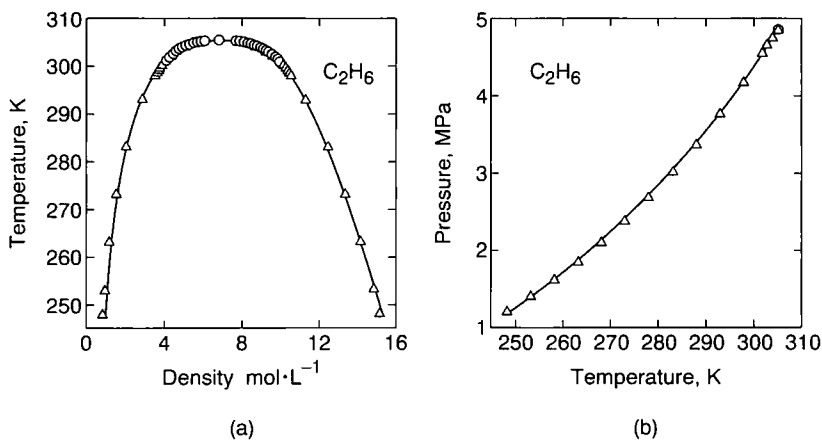


Fig. 8. Densities (a) and saturation pressures (b) of the coexisting vapor and liquid phases of ethane below the critical temperature. The symbols represent experimental density data [41, 43] and experimental vapor-pressure data [41]. The curves represent the values calculated with the crossover equation of state.

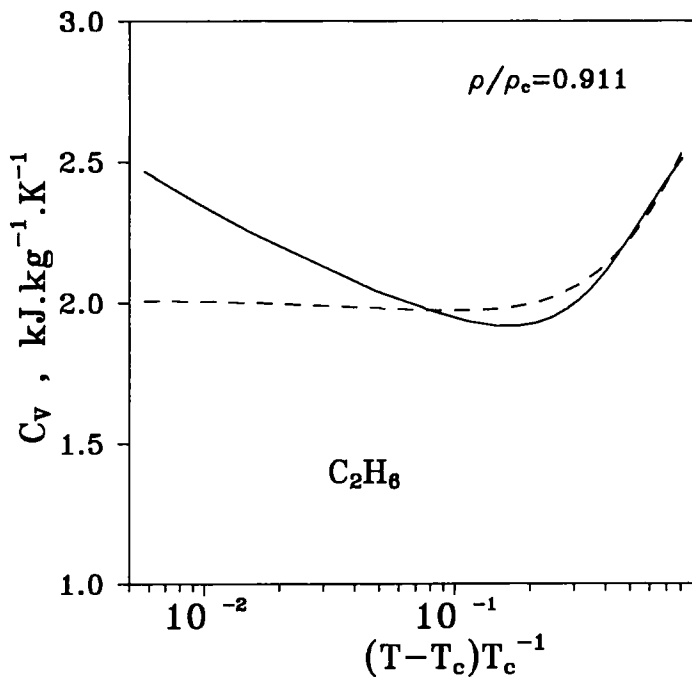


Fig. 9. Isochoric specific heat capacity C_v of ethane as a function of temperature. The solid curves represent values calculated with the crossover equation, and the dashed curves values calculated with NIST14 [24].

The experimental C_V data of Shmakov [42] are limited to temperatures within $|\tau| < 0.1$. We found that by changing the caloric background parameters $\tilde{\mu}_j^{(2)}$ we could get an equally good representation of these experimental C_V data while obtaining better consistency with the values for the specific heat capacity calculated with NIST14 farther away from the critical temperature as indicated in Fig. 9. The values adopted for the system-dependent constants for ethane are included in Table II. The coefficient $\tilde{\mu}_1^{(2)} \neq 0$ was selected by a procedure discussed in the next section. In terms of reduced temperatures and densities the range of validity of the crossover equation for ethane is approximately the same as the range for methane given by Eq. (26).

5. APPLICATION TO MIXTURES

In order to apply the crossover equation of state to mixtures we need the critical parameters $T_c(\zeta)$, $P_c(\zeta)$, and $\rho_c(\zeta)$ as a function of the field variable ζ . However, the actual experimental information for these parameters is available only as a function of the concentration x . The variable x is to be converted into the variable ζ by using Eq. (14). However, for this purpose we need \hat{A}_{eff} , which in turn depends on $T_c(\zeta)$, $P_c(\zeta)$, and $\rho_c(\zeta)$. Although it is possible to go through this procedure [9, 18], the procedure becomes much simpler if the field variable ζ is selected such that at the critical locus it becomes numerically equal to the mole fraction x :

$$x = \zeta \quad \text{for} \quad T = T_c, \quad P = P_c, \quad \rho = \rho_c \quad (28)$$

We refer to this condition as the critical-line condition (CLC) and it has been introduced by many investigators [8, 10, 11, 44–52]. The experimentally accessible thermodynamic properties of the mixture will be independent of the zero point of the entropy and energy selected for the two pure-fluid components and, hence, independent of the coefficient $\tilde{\mu}_0^{(1)}$, $\tilde{\mu}_0^{(2)}$, $\tilde{\mu}_1^{(1)}$, and $\tilde{\mu}_1^{(2)}$. However, the hidden field ζ and the ordering field h will actually depend on the choices adopted for the zero points of entropy and energy as follows from Eq. (5). We can use the freedom of choice of the zero points in part in an attempt to satisfy the CLC as required by Eq. (28). Nevertheless, for the variables adopted in this paper, it is impossible to satisfy the CLC exactly and it introduces an approximation as discussed by Anisimov and Sengers [11]. For mixtures of carbon dioxide and ethane the CLC has been shown to be a good approximation [9, 18] and we

adopt the CLC for mixtures of methane and ethane also. Substitution of Eq. (14) with Eq. (28) yields for the CLC

$$x = \zeta - \frac{\zeta(1-\zeta)}{\rho_c(\zeta) R} G(\zeta) \quad (29)$$

with

$$G(\zeta) = [\tilde{A}_0(\zeta) + \tilde{\mu}_0(\zeta)] \frac{d(P_c/T_c)}{d\zeta} - \frac{P_c(\zeta)}{\rho_c(\zeta) T_c(\zeta)} \frac{d\rho_c}{d\zeta} \tilde{\mu}_0(\zeta) + \frac{P_c(\zeta)}{T_c(\zeta)} \frac{d\tilde{\mu}_0}{d\zeta} - [\tilde{A}_1(\zeta) + \tilde{\mu}_1(\zeta)] \frac{P_c(\zeta)}{T_c^2(\zeta)} \frac{dT_c}{d\zeta} \quad (30)$$

We note that Eq. (30) corrects Eq. (4.12) in Ref. 8. The CLC requires that

$$G(\zeta) = 0 \quad \text{for } T = T_c, \quad P = P_c, \quad \rho = \rho_c \quad (31)$$

To implement the CLC we find it convenient to define

$$\tilde{\mu}'_0(\zeta) = Z_c(\zeta) \mu_0(\zeta) \quad (32)$$

where $Z_c(\zeta) = P_c(\zeta)/\rho_c(\zeta) RT_c(\zeta)$. Equation (30) then reduces to

$$G(\zeta) = R\rho_c(\zeta) \frac{d\tilde{\mu}'_0}{d\zeta} - \frac{P_c(\zeta)}{T_c^2(\zeta)} \frac{dT_c}{d\zeta} [\tilde{A}_1(\zeta) + \tilde{\mu}_1(\zeta)] - \frac{d(P_c/T_c)}{d\zeta} \quad (33)$$

The CLC condition is satisfied if we demand that

$$\frac{d\tilde{\mu}'_0(\zeta)}{d\zeta} = \frac{P_c(\zeta)}{R\rho_c(\zeta) T_c^2(\zeta)} \frac{dT_c}{d\zeta} [\tilde{A}_1(\zeta) + \tilde{\mu}_1(\zeta)] + \frac{1}{R\rho_c(\zeta)} \frac{d(P_c/T_c)}{d\zeta} \quad (34)$$

The expressions for the pressure, the specific heat capacities and the speed of sound of the mixture do not depend on $\tilde{\mu}'_0(\zeta)$ directly, but only on its first and second derivatives with respect to ζ . These derivatives can be calculated readily from Eq. (34). However, to calculate the excess enthalpy, one needs $\tilde{\mu}'_0(\zeta)$ which is to be obtained by integrating Eq. (34), as was done by Jin et al. [8] for mixtures of carbon dioxide and ethane.

In principle, there are a number of different ways in which one can implement the CLC as expressed by Eq. (31). In applying a scaled cross-over equation of state to mixtures of carbon dioxide and ethane, Jin et al. [8] took $\tilde{\mu}_1(\zeta) = -\tilde{A}_1(\zeta)$ and then calculated $\tilde{\mu}_0(\zeta)$ from Eq. (34). The CLC as applied here is similar to the way the CLC was previously

implemented by Povodyrev et al. for a representation of the thermodynamic properties of methane and ethane in terms of a parametric scaled equation of state for the asymptotic critical thermodynamic behavior [51]. The internal energy density $\hat{u} = U/V$ and the entropy density $\hat{s} = S/V$ on the critical line are given by

$$\hat{u}_c(x) = -P_c(x)[\tilde{A}_1(x) + \tilde{\mu}_1(x)] \quad (35)$$

$$\hat{s}_c(x) = \frac{\hat{u}_c(x)}{T_c(x)} + \frac{P_c(x)}{T_c(x)} - \rho_c(x)R[\tilde{\mu}'_0(x) + x \ln x + (1-x) \ln(1-x)] \quad (36)$$

From Eq. (35) we see that the choice $\tilde{\mu}_1 = -\tilde{A}_1(\zeta)$ implies that $\hat{u}_c = 0$ everywhere along the critical locus [8]. In the present approach $\tilde{\mu}_1(\zeta)$ is left free but $\tilde{\mu}_0(\zeta)$ and, hence, $\hat{s}_c(x)$ is restricted by the solution of Eq. (34).

To specify the crossover equation for \tilde{A}_{eff} of the mixture, we also need the system-dependent parameters $\tilde{u}(\zeta)$, $A(\zeta)$, $c_r(\zeta)$, $c_p(\zeta)$, $c(\zeta)$, $d_1(\zeta)$, $a_{jk}(\zeta)$, $\tilde{A}_j(\zeta)$, and $\tilde{\mu}_j(\zeta)$ for $j \geq 3$, to be designated $k_j(\zeta)$, as a function of the variable ζ . In the case of mixtures of carbon dioxide and ethane, it was possible to interpolate all system-dependent $k_j(\zeta)$ linearly between $k_j^{(1)}$ for $\zeta = 0$ and $k_j^{(2)}$ for $\zeta = 1$, except for the background coefficient $\tilde{\mu}_2(\zeta)$ [9, 18]. However, methane and ethane have significantly different critical temperatures and a simple linear interpolation will not be adequate. Following the earlier work of Kiselev and co-workers [50, 51], we assume that $k_j(\zeta)$ will depend on ζ primarily through the isomorphous critical compressibility factor $Z_c(\zeta)$, which is written in the form

$$Z_c(\zeta) = (1 - \zeta) Z_c^{(1)} + \zeta Z_c^{(2)} + \Delta Z_c(\zeta) \quad (37)$$

where $Z_c^{(1)}$ and $Z_c^{(2)}$ are the critical compressibility factors of methane and ethane, respectively. We then represent the system-dependent coefficients $k_j(\zeta)$ in the crossover equation of state by interpolation functions of the form

$$k_j(\zeta) = (1 - \zeta) k_j^{(1)} + \zeta k_j^{(2)} + k_j^{(m)} \Delta Z_c(\zeta) \quad (38)$$

where $k_j^{(m)}$ are mixing coefficients to be determined by fits to available thermodynamic property data for the mixtures.

As mentioned earlier, the coefficient $\tilde{\mu}_0(\zeta)$ is determined implicitly by Eqs. (32) and (34). In the equation for $\tilde{\mu}_1(\zeta)$

$$\tilde{\mu}_1(\zeta) = (1 - \zeta) \tilde{\mu}_1^{(1)} + \zeta \tilde{\mu}_1^{(2)} + \tilde{\mu}_1^{(m)} \Delta Z_c(\zeta) \quad (39)$$

we arbitrarily took $\tilde{\mu}_1^{(1)} = 0$ for methane, but the coefficient $\tilde{\mu}_1^{(2)}$ for ethane and the mixing coefficient $\tilde{\mu}_1^{(m)}$ were left as adjustable parameters.

6. MIXTURES OF METHANE AND ETHANE

We have applied our scaled crossover equation for the effective isomorphic Helmholtz free-energy density to represent experimental thermodynamic-property data for mixtures of methane and ethane. To determine the system-dependent parameters in the crossover equation we have used the following experimental information:

- (i) experimental P - ρ - T - x data obtained by Haynes et al. [53] for three concentrations (0.31474, 0.49783, and 0.65472 mole fractions of ethane);
- (ii) experimental P - ρ - T - x data obtained by Bespalov et al. [54] for three concentrations (0.0986, 0.3995, and 0.84 mole fractions of ethane);
- (iii) experimental specific heat capacities obtained by Nagaev et al. [55] for three concentrations (0.0986, 0.3995, and 0.84 mole fractions of ethane); and
- (iv) experimental specific heat capacities obtained by Mayrath and Magee [56] for three concentrations (0.31474, 0.49783, and 0.65472 mole fractions of ethane).

Furthermore, to extend the range of validity of the crossover equation for mixtures to higher temperatures we have supplemented the experimental $C_{V,x}$ data with $C_{V,x}$ values calculated from NIST14 [24]. The range of temperatures and densities of the data used in the analysis is shown in Fig. 10.

We also need equations for the critical temperature $T_c(\zeta)$, the critical density $\rho_c(\zeta)$, and the critical pressure $P_c(\zeta)$ as functions of the hidden field ζ . Since along the critical line $\zeta = x$, the quantities $T_c(\zeta)$, $\rho_c(\zeta)$, and $P_c(\zeta)$ depend on ζ in the same way as on x , it follows that

$$T_c(\zeta) = T_c(x), \quad \rho_c(\zeta) = \rho_c(x), \quad P_c(\zeta) = P_c(x) \quad (40)$$

In practice, we represent the critical parameters of the mixtures by polynomials of the form [8]

$$T_c(x) = T_c^{(1)}(1-x) + T_c^{(2)}x + (T_1 + T_2x + T_3x^2)x(1-x) \quad (41)$$

$$\frac{1}{\rho_c(x)} = \frac{1}{\rho_c^{(1)}}(1-x) + \frac{1}{\rho_c^{(2)}}x + (v_1 + v_2x + v_3x^2)x(1-x) \quad (42)$$

$$\frac{P_c(x)}{RT_c(x)} = \frac{P_c^{(1)}}{RT_c^{(1)}}(1-x) + \frac{P_c^{(2)}}{RT_c^{(2)}}x + (P_1 + P_2x + P_3x^2)x(1-x) \quad (43)$$

where x is the concentration of ethane and where $T_c^{(i)}$, $\rho_c^{(i)}$, and $P_c^{(i)}$ are the critical parameters of methane ($i = 1$) and ethane ($i = 2$).

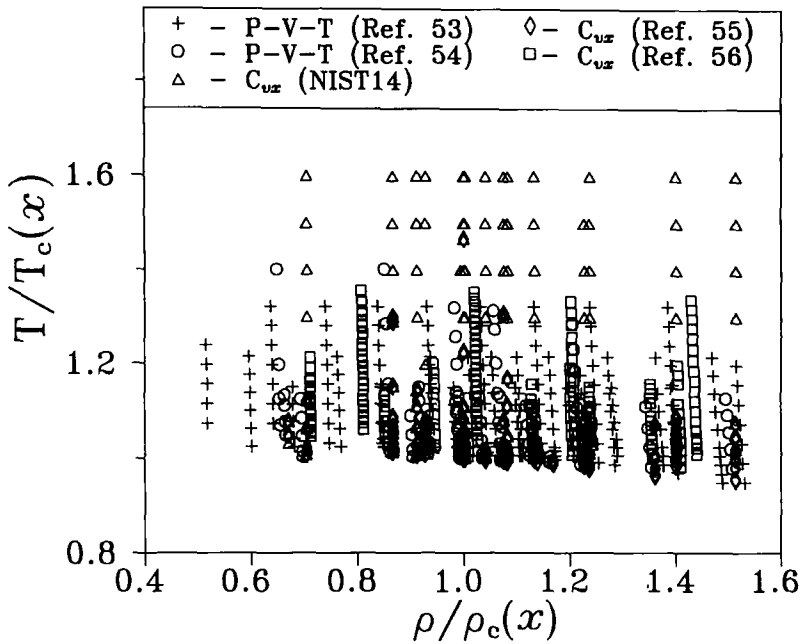
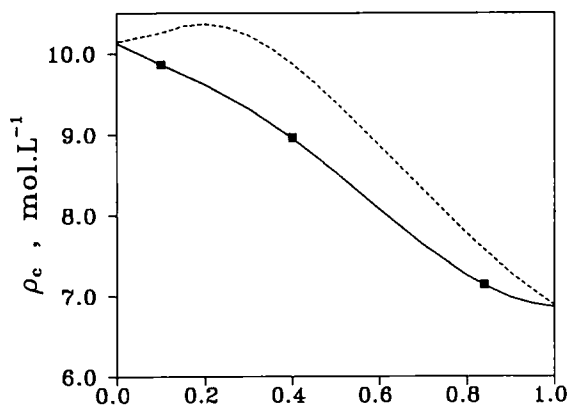
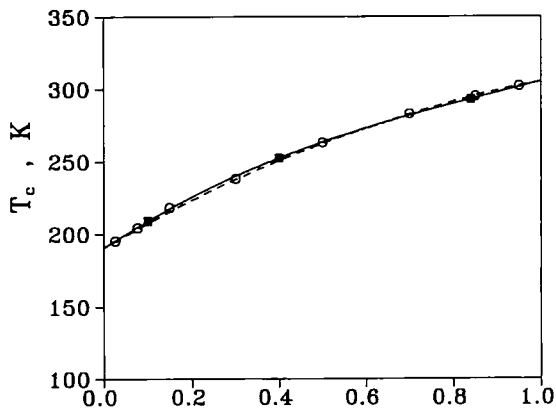


Fig. 10. Temperatures and densities of the thermodynamic-property values used in the determination of the system-dependent parameters in the crossover equation for mixtures of methane and ethane.

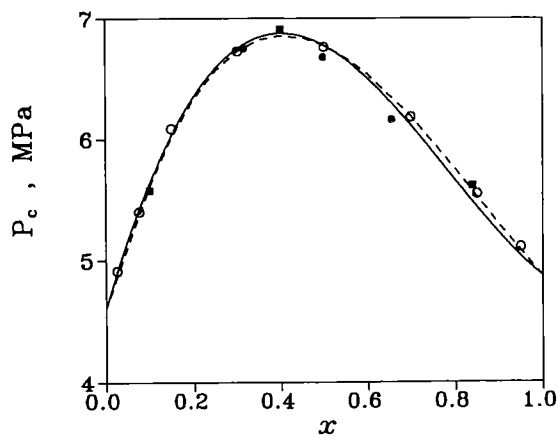
For the determination of the coefficients P_i in Eq. (43) we used the experimental data of Ellington et al. [57], which appear to be in good agreement with the P - ρ - T - x data of Bespalov et al. [54]. However, the analytic equation of state, proposed by Haynes et al. [53] for mixtures of methane and ethane, predicts different values for the critical pressures calculated at $T = T_c(x)$ and $\rho = \rho_c(x)$. Therefore, we determined the coefficients P_1 , P_2 , and P_3 in Eq. (43) for the critical pressures and the mixing coefficients $k_j^{(m)}$ in Eq. (38) from a fit to both sets of experimental P - ρ - T - x data. For the determination of the coefficients T_1 , T_2 , and T_3 in Eq. (41) for the critical temperature the experimental data obtained by Kiselev et al. [58] were used as initial values. However, Kiselev et al. [58] have reported critical temperatures for three concentrations only, which is not enough for a determination of all adjustable coefficients in Eq. (41). Therefore we determined the coefficients T_i together with the background coefficients $\tilde{\mu}_i(\zeta)$ ($i = 1-5$) from a fit to the experimental $C_{V,x}$ data of Nagaev et al. [55] and of Mayrath and Magee [56]. For the determination of the



(a)



(b)



(c)

coefficients v_1 , v_2 , and v_3 in Eq. (42) for the critical density, we again started by using the experimental data of Kiselev et al. [58] as initial values. In the final stage the coefficients in Eqs. (41)–(43) for the critical parameters and the mixing coefficients $k_j^{(m)}$ in the crossover equation of state were determined from a fit to all sets of experimental P – ρ – T – x and $C_{V,x}$ data simultaneously. The values of the coefficients in Eqs. (41)–(43) for the critical parameters are presented in Table III. The critical parameters are shown in Fig. 11 as a functions of x . Equation (41) reproduces the critical temperatures of Kiselev et al. [58] to within 0.03 K, their critical densities to within 0.01 mol · L⁻¹, and their critical pressures to within 0.05 MPa.

As mentioned in the preceding section to represent the coefficients $c_r(\zeta)$, $c_\rho(\zeta)$, $\tilde{A}_j(\zeta)$ for $j = 1, 2, 3$ and $\tilde{\mu}_j(\zeta)$ for $j \geq 1$, we used Eq. (38) with $k_j^{(m)} \neq 0$. For the crossover parameters $\tilde{u}(\zeta)$ and $A(\zeta)$, the scaling-field parameters $c(\zeta)$ and $d_1(\zeta)$, the classical Landau-expansion parameters $a_{jk}(\zeta)$ and the background coefficient $\tilde{A}_4(\zeta)$, linear interpolation formulae with $k_j^{(m)} = 0$ appeared to be adequate.

The available experimental $C_{V,x}$ data [55, 56] are restricted to temperatures $T \leq 1.4T_c(x)$. To extend the range of validity of our crossover equation of state, we supplemented the experimental $C_{V,x}$ data with values from the NIST14 program developed by Friend and co-workers [23–25] at temperatures up to $T = 1.6T_c(x)$. This analytic equation cannot describe the thermodynamic properties of the mixtures in the near-critical region, but farther away from the critical point it represents experimental specific heat capacities [56] and experimental speed-of-sound data [62] within

Fig. 11. (a) Critical density of methane + ethane mixtures as a function of concentration. The filled symbols indicate experimental data obtained by Kiselev et al. [58], the dashed line corresponds to values calculated with an equation proposed by Rainwater [10], and the solid curve represents values calculated with Eq. (42). (b) Critical temperature of methane + ethane mixtures as a function of concentration. The filled symbols indicate experimental data obtained by Kiselev et al. [58], the circles indicate experimental data obtained by Bloomer et al. [59], the dashed line corresponds to values calculated with an equation proposed by Rainwater [10], and the solid curve represents values calculated with Eq. (41). (c) Critical pressure of methane + ethane mixtures as a function of concentration. The filled squares indicate experimental data obtained by Kiselev et al. [58], the circles indicate experimental data obtained by Bloomer et al. [59], the filled circles correspond to values calculated with an analytical equation proposed by Haynes et al. [53], the dashed line corresponds to values calculated with equation proposed by Rainwater [10], and the solid curve represents values calculated with Eq. (43).

Table III. Critical-Line Parameters for $\text{CH}_4 + \text{C}_2\text{H}_6$

Temperature (K)
$T_c^{(1)} = 190.564$
$T_c^{(2)} = 305.322$
$T_1 = 83.206$
$T_2 = -34.869$
$T_3 = -13.350$
Density ($\text{mol} \cdot \text{L}^{-1}$)
$\rho_c^{(1)} = 10.122$
$\rho_c^{(2)} = 6.8592$
$v_1 = -0.017090$
$v_2 = -0.070526$
$v_3 = 0.12909$
Pressure ($\text{MPa} \cdot \text{mol} \cdot \text{kJ}^{-1}$)
$P_c^{(1)}/RT_c^{(1)} = 2.9028$
$P_c^{(2)}/RT_c^{(2)} = 1.9191$
$P_1 = 5.624$
$P_2 = -7.1191$
$P_3 = 2.786$

3% [23]. To apply our crossover equation to temperatures larger than $T = 1.4T_c(x)$ we introduced two additional coefficients, $\tilde{\mu}_6(\zeta)$ and $\tilde{\mu}_7(\zeta)$ for the mixtures. The values for the mixing coefficients $k_j^{(m)}$ are included in Table II.

In Fig. 12 we show a comparison of the pressures calculated from the crossover equation of state with the experimental pressure data of Bespalov et al. [54] and those of Haynes et al. [53]. As mentioned earlier, the two data sets correspond to slightly different critical pressures. Our crossover equation of state essentially amounts to a compromise between the two data sets.

A comparison with the experimental $C_{v,x}$ data of Nagaev et al. [55] and with those of Mayrath and Magee [56] is presented in Fig. 13. In the temperature range $0.97T_c(x) \leq T \leq 1.4T_c(x)$ and density range $0.7\rho_c(x) \leq \rho \leq 1.5\rho_c(x)$, the deviations of the experimental values from the calculated values are within 5% mostly. However, the data in Ref. [56] at $\rho/\rho_c \leq 0.81$ show deviations up to 10%, indicating some differences between the two data sets.

The paper of Nagaev et al. [56] also includes some experimental coexistence-curve data which are well represented by our crossover equation of state as shown in Fig. 14. A comparison with the experimental dew and bubble-point data obtained by Bloomer et al. [59] is shown in Fig. 15.

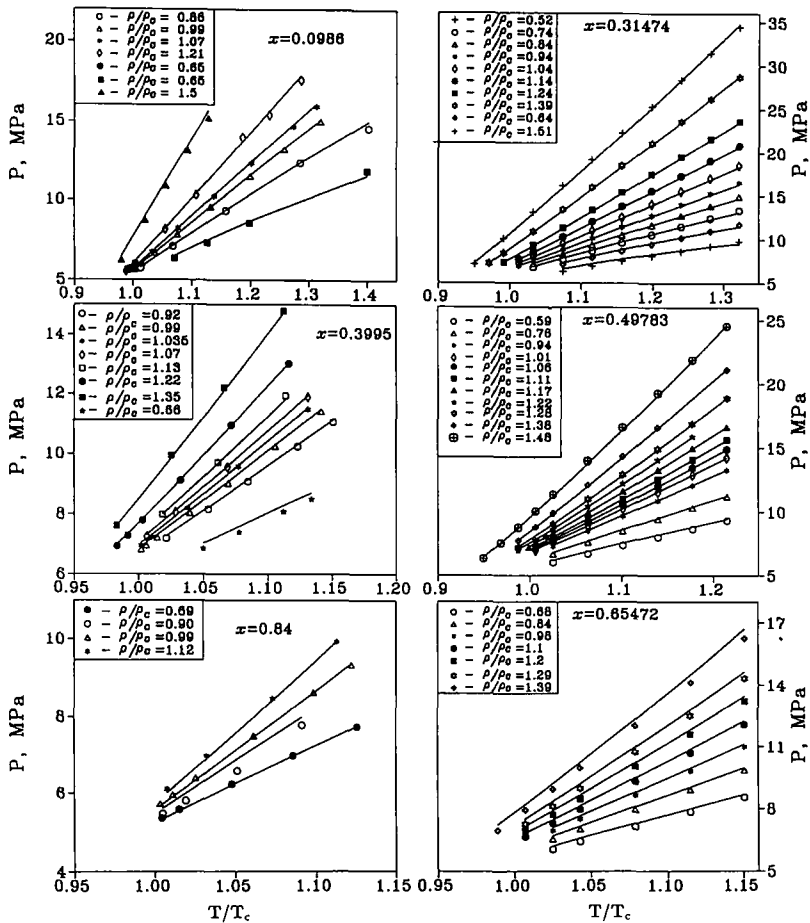


Fig. 12. The pressure of methane + ethane mixtures at concentrations $x = 0.0986$, $x = 0.3995$, $x = 0.84$, $x = 0.31474$, $x = 0.49783$, and $x = 0.65472$ mole fraction of ethane as a function of temperature. The symbols indicate the experimental data obtained by Bespalov et al. [54] and by Haynes et al. [53] and the curves represent values calculated with the crossover model. The solid curves represent values calculated with the crossover equation.

There are systematic deviations between the experimental and the calculated values in the vapor branch at $x = 0.1484$ and on the liquid branches at $x = 0.6998$ and $x = 0.8493$. While our crossover equation is valid in a large temperature range above $T_c(x)$, it still has a somewhat limited validity near the phase boundary below $T_c(x)$. A comparison of our crossover equation with the experimental vapor-liquid equilibrium data

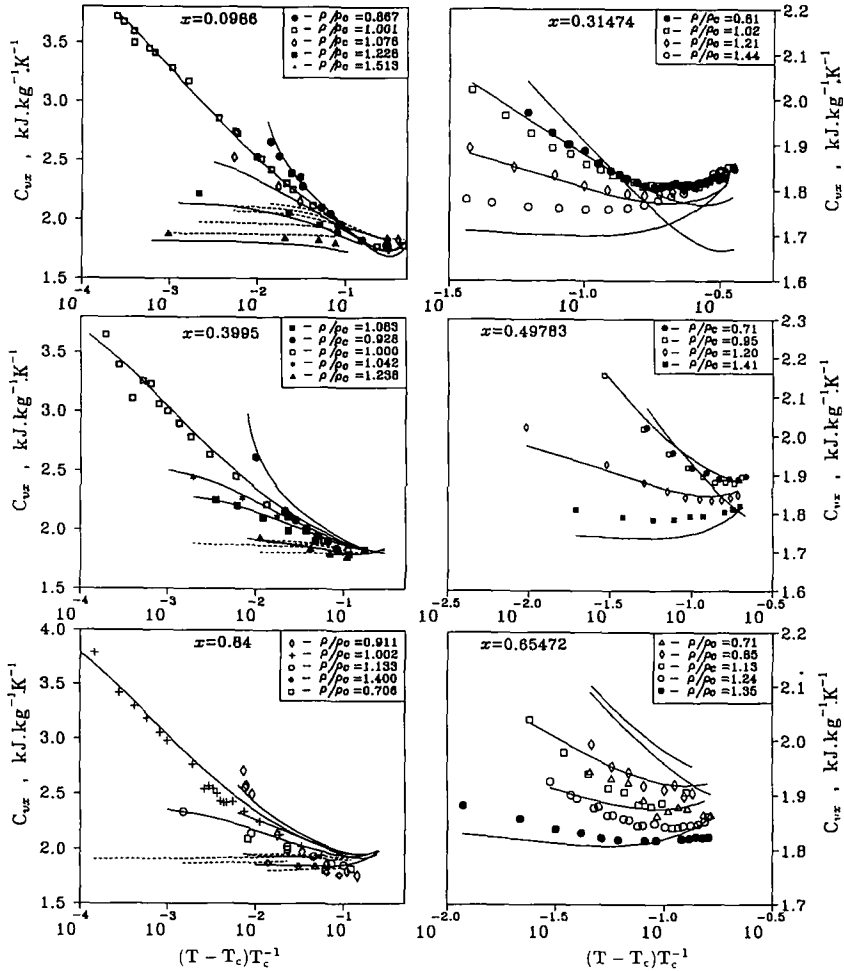


Fig. 13. Isochoric specific heat $C_{v,x}$ of methane+ethane mixtures at concentrations $x = 0.0986$, $x = 0.3995$, $x = 0.84$, $x \approx 0.31474$, $x \approx 0.49783$, and $x = 0.65472$ mole fraction of ethane as a function of temperature. The symbols indicate experimental data obtained by Nagaev et al. [55] and by Mayrath and Magee [56]. The solid curves represent values calculated with the crossover model and the dashed curves values calculated with NIST14 [24].

obtained by Wichterle and Kobayashi [60] and Davalos et al. [61] is presented in Figs. 16 and 17. Our crossover equation yields a satisfactory representation of these vapor-liquid equilibrium data.

More recently, Younglove et al. [62] have reported speed-of-sound measurements for mixtures of methane and ethane. Most of the experimental

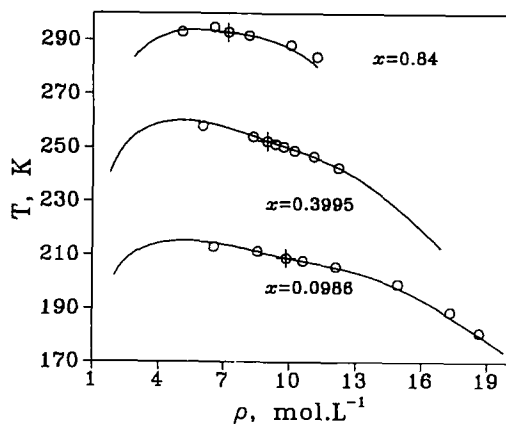


Fig. 14. Densities of the coexisting vapor and liquid phase of methane as a function of temperature at constant concentration. The symbols indicate the experimental data obtained by Nagaev et al. [55] and the curves represents values calculated with the cross-over model.

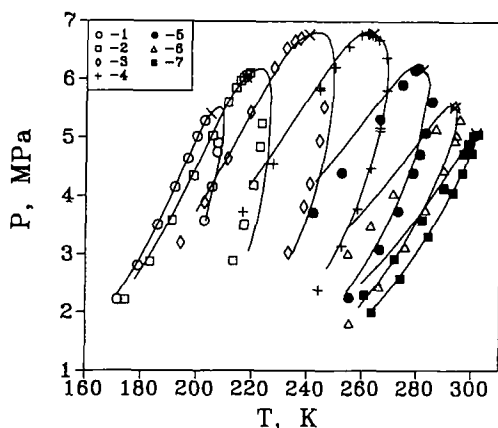


Fig. 15. Dew and bubble-point diagrams at constant concentration. The symbols indicate the experimental data obtained by Bloomer et al. [59] [(1) $x=0.075$, (2) $x=0.1484$, (3) $x=0.3$, (4) $x=0.4998$, (5) $x=0.6998$, (6) $x=0.8493$, and (7) $x=0.95$ mole fraction of ethane] and the curves represent values calculated with the crossover model.

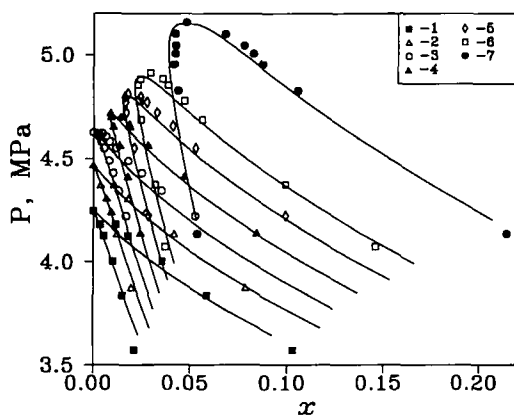


Fig. 16. The pressure–composition diagram for ethane + methane mixtures. The symbols indicate experimental data obtained by Wichterle and Kobayashi [60] [(1) $T=188.04$ K, (2) $T=189.65$ K, (3) $T=190.94$ K, (4) $T=192.39$ K, (5) $T=193.92$ K, (6) $T=195.44$ K, and (7) $T=199.92$ K] and the curves represent values calculated with the crossover model.

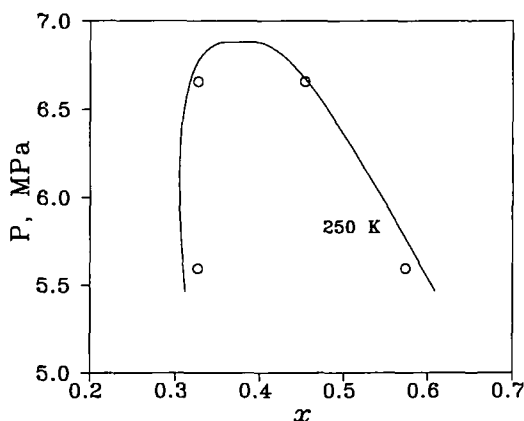


Fig. 17. The pressure–composition diagram for ethane + methane mixtures. The symbols indicate experimental data obtained by Davalos et al. [61] and the curve represents values calculated with the crossover model.

data are outside the range of validity of our crossover equation, which is not adequate for densities smaller than $0.6 \rho_c(x)$. A comparison with the experimental sound velocities of Younglove et al. inside the range of validity of our crossover equation is shown in Fig. 18. The deviations are of the order of 6%.

7. DISCUSSION

Guided by the modern theory of critical phenomena in one-component fluids and based on the isomorphism principle for its extension to fluid mixtures, we have presented a crossover equation for the thermodynamic properties of mixtures of methane and ethane that incorporates theoretically predicted singular thermodynamic behavior in the vicinity of the critical line and recovers regular classical thermodynamic behavior far away from the critical line. The crossover equation is valid in the temperature range $0.97T_c(x) \leq T \leq 1.6T_c(x)$ at $\rho = \rho_c(x)$ and in the density range $0.7\rho_c(x) \leq \rho \leq 1.5\rho_c(x)$ at $T = T_c(x)$. The pressures are well represented down to $0.9T_c$ at $\rho = \rho_c(x)$ and down to $0.5 \rho_c(x)$ at $T = T_c(x)$. In applying the isomorphism principle we have employed an ordering field h where the conjugate thermodynamic variable, serving as the ordering parameter, is the density at constant chemical potential. In principle we may consider an ordering field h that is a more general function of the physical fields μ_1 , μ_2 , and T . As pointed out by Anisimov et al. [63, 64], the introduction of a more general ordering field is necessary if we want to account for crossover from vapor–liquid critical behavior to liquid–liquid critical behavior. Such a more general isomorphism approach may also potentially lead to a more accurate crossover equation of state for mixtures like mixtures of methane and ethane which do not exhibit crossover from vapor–liquid critical behavior to liquid–liquid critical behavior. However, a crossover equation of state based on such a more general ordering field, and hence a more general order parameter, has not yet been developed.

APPENDIX A: RELEVANT THERMODYNAMIC DERIVATIVES

Derivatives of Free-Energy Density

$$\left[\frac{\partial \Delta \tilde{A}}{\partial \Delta \tilde{p}} \right]_{\tau, \zeta} = c_p(\zeta) \left[\frac{\partial \Delta \tilde{A}_r}{\partial M} \right]_{t, \zeta} \quad (\text{A1})$$

$$\left[\frac{\partial \Delta \tilde{A}}{\partial \tau} \right]_{\Delta \tilde{p}, \zeta} = c_t(\zeta) \left[\frac{\partial \Delta \tilde{A}_r}{\partial t} \right]_{M, \zeta} - c_p(\zeta) d_1(\zeta) \left[\frac{\partial \Delta \tilde{A}_r}{\partial M} \right]_{t, \zeta} \quad (\text{A2})$$

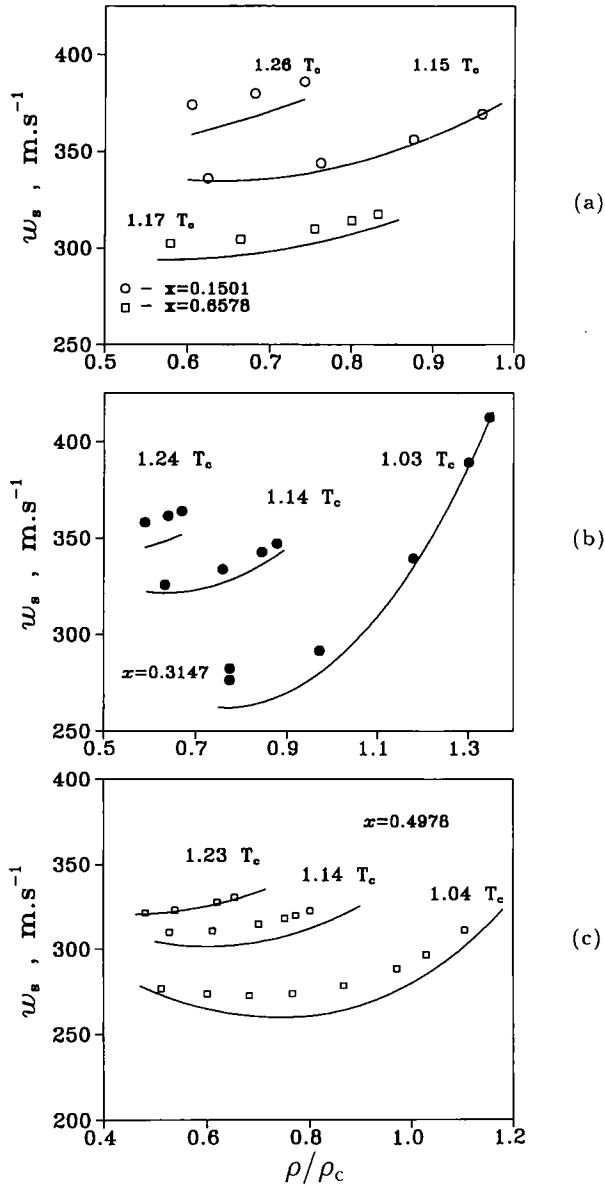


Fig. 18. The speed of sound of methane+ethane mixtures at constant concentrations as a function of density. The symbols indicate experimental data obtained by Younglove et al. [62] and the curves represent values calculated with the crossover model.

$$\left[\frac{\partial^2 \Delta \tilde{A}}{\partial \Delta \tilde{p}^2} \right]_{\tau, \zeta} = c_\rho^2(\zeta) \left[\frac{\partial^2 \Delta \tilde{A}_r}{\partial M^2} \right]_{\tau, \zeta} \tilde{G}^{-1} \tag{A3}$$

$$\begin{aligned} \frac{\partial^2 \Delta \tilde{A}}{\partial \Delta \tilde{p} \partial \tau} &= c_\rho(\zeta) c_\tau(\zeta) \left\{ \frac{\partial^2 \Delta \tilde{A}_r}{\partial t \partial M} - c(\zeta) \left(\left[\frac{\partial^2 \Delta \tilde{A}_r}{\partial t \partial M} \right]^2 \right. \right. \\ &\quad \left. \left. - \left[\frac{\partial^2 \Delta \tilde{A}_r}{\partial t^2} \right]_{M, \zeta} \left[\frac{\partial^2 \Delta \tilde{A}_r}{\partial M^2} \right]_{\tau, \zeta} \right) \right\} \tilde{G}^{-1} \\ &\quad - c_\rho^2(\zeta) d_1(\zeta) \left[\frac{\partial^2 \Delta \tilde{A}_r}{\partial M^2} \right]_{\tau, \zeta} \tilde{G}^{-1} \end{aligned} \tag{A4}$$

$$\begin{aligned} \left[\frac{\partial^2 \Delta \tilde{A}}{\partial \tau^2} \right]_{\Delta \tilde{p}, \zeta} &= c_\tau^2(\zeta) \left[\frac{\partial^2 \Delta \tilde{A}_r}{\partial t^2} \right]_{M, \zeta} \tilde{G}^{-1} - 2c_\tau(\zeta) c_\rho(\zeta) d_1(\zeta) \\ &\quad \times \left\{ \frac{\partial^2 \Delta \tilde{A}_r}{\partial t \partial M} - c(\zeta) \left(\left[\frac{\partial^2 \Delta \tilde{A}_r}{\partial t \partial M} \right]^2 \right. \right. \\ &\quad \left. \left. - \left[\frac{\partial^2 \Delta \tilde{A}_r}{\partial t^2} \right]_{M, \zeta} \left[\frac{\partial^2 \Delta \tilde{A}_r}{\partial M^2} \right]_{\tau, \zeta} \right) \right\} \tilde{G}^{-1} \\ &\quad + c_\rho^2(\zeta) d_1^2(\zeta) \left[\frac{\partial^2 \Delta \tilde{A}_r}{\partial M^2} \right]_{\tau, \zeta} \tilde{G}^{-1} \end{aligned} \tag{A5}$$

with

$$\tilde{G} = \left[1 - c(\zeta) \frac{\partial^2 \Delta \tilde{A}_r}{\partial t \partial M} \right]^2 - c^2(\zeta) \left[\frac{\partial^2 \Delta \tilde{A}_r}{\partial t^2} \right]_{M, \zeta} \left[\frac{\partial^2 \Delta \tilde{A}_r}{\partial M^2} \right]_{\tau, \zeta} \tag{A6}$$

Derived Thermodynamic Quantities

Pressure P and its derivatives:

$$\frac{P}{RT} = \hat{P} = \rho \left[\frac{\partial \hat{A}}{\partial \rho} \right]_{\tau, \zeta} - \hat{A}_{\text{eff}}(\tau, \rho, \zeta) \tag{A7}$$

$$\frac{1}{RT} \left[\frac{\partial P}{\partial T} \right]_{\rho, x} = \frac{\hat{P}}{T} + \left[\frac{\partial \hat{P}}{\partial T} \right]_{\rho, \zeta} - \left[\frac{\partial \hat{P}}{\partial \zeta} \right]_{\rho, T} \left[\frac{\partial x}{\partial T} \right]_{\rho, \zeta} \left[\frac{\partial \zeta}{\partial x} \right]_{\rho, T} \tag{A8}$$

$$\frac{1}{RT} \left[\frac{\partial P}{\partial \rho} \right]_{\tau, x} = \left[\frac{\partial \hat{P}}{\partial \rho} \right]_{\tau, \zeta} - \left[\frac{\partial \hat{P}}{\partial \zeta} \right]_{\rho, T} \left[\frac{\partial x}{\partial \rho} \right]_{\tau, \zeta} \left[\frac{\partial \zeta}{\partial x} \right]_{\rho, T} \tag{A9}$$

Isochoric specific heat capacity $C_{v,x}$ per mole:

$$\begin{aligned} \frac{\rho C_{v,x}}{R} = & -\frac{T_c^2(\zeta)}{T^2} \left[\frac{\partial^2 \hat{A}_{\text{eff}}}{\partial \tau^2} \right]_{\rho, \zeta} \\ & + \left\{ \frac{dT_c}{d\zeta} \left[\frac{\partial \hat{A}_{\text{eff}}}{\partial \tau} \right]_{\rho, \zeta} + T_c \frac{\partial^2 \tilde{A}_{\text{eff}}}{\partial \tau \partial \zeta} - \frac{T_c}{T} \frac{dT_c}{d\zeta} \left[\frac{\partial^2 \tilde{A}_{\text{eff}}}{\partial \tau^2} \right]_{\rho, \zeta} \right\} \\ & \times \left[\frac{\partial \zeta}{\partial x} \right]_{\rho, T} \left[\frac{\partial x}{\partial T} \right]_{\rho, \zeta} \end{aligned} \tag{A10}$$

Isobaric specific heat capacity $C_{p,x}$ per mole:

$$\frac{\rho(C_{p,x} - C_{v,x})}{R} = \left\{ \hat{P} + T \left[\frac{\partial \hat{P}}{\partial T} \right]_{\rho, x} \right\}^2 \frac{1}{\rho} \left[\frac{\partial \hat{P}}{\partial \rho} \right]_{T, x}^{-1} \tag{A11}$$

Speed of sound:

$$w_s = \left\{ \left[\frac{\partial P}{\partial \rho} \right]_{T, x} \frac{C_{p,x}}{C_{v,x}} \right\}^{1/2} \tag{A12}$$

Derivatives of the concentration x :

$$\left[\frac{\partial x}{\partial \zeta} \right]_{\rho, T} = 1 - \frac{1}{\rho} (1 - 2\zeta) \left[\frac{\partial \hat{A}_{\text{eff}}}{\partial \zeta} \right]_{\rho, T} - \frac{1}{\rho} \zeta (1 - \zeta) \left[\frac{\partial^2 \hat{A}_{\text{eff}}}{\partial \zeta^2} \right]_{\rho, T} \tag{A13}$$

$$\begin{aligned} \frac{T^2}{T_c} \left[\frac{\partial x}{\partial T} \right]_{\rho, \zeta} = & -\frac{1}{\rho} \zeta (1 - \zeta) \left\{ \frac{\partial^2 \hat{A}_{\text{eff}}}{\partial \zeta \partial \tau} - \frac{1}{T} \frac{dT_c}{d\zeta} \right. \\ & \left. \times \left[\frac{\partial^2 \hat{A}_{\text{eff}}}{\partial \tau^2} \right]_{\rho, \zeta} + \frac{1}{T_c} \frac{dT_c}{d\zeta} \left[\frac{\partial \hat{A}_{\text{eff}}}{\partial \tau} \right]_{\rho, \zeta} \right\} \end{aligned} \tag{A14}$$

$$\left[\frac{\partial x}{\partial \rho} \right]_{T, \zeta} = \frac{1}{\rho} \zeta (1 - \zeta) \left\{ \frac{1}{\rho} \left[\frac{\partial \hat{A}_{\text{eff}}}{\partial \zeta} \right]_{\rho, T} - \frac{\partial^2 \hat{A}_{\text{eff}}}{\partial \zeta \partial \rho} + \frac{1}{T} \frac{dT_c}{d\zeta} \frac{\partial^2 \hat{A}_{\text{eff}}}{\partial \tau \partial \rho} \right\} \tag{A15}$$

Note: the derivatives:

$$\left[\frac{\partial \hat{A}_{\text{eff}}}{\partial \zeta} \right]_{\rho, T}, \left[\frac{\partial^2 \hat{A}_{\text{eff}}}{\partial \zeta^2} \right]_{\rho, T}, \frac{\partial^2 \hat{A}_{\text{eff}}}{\partial \zeta \partial \rho}, \frac{\partial^2 \hat{A}_{\text{eff}}}{\partial \zeta \partial \tau} \tag{A16}$$

have been evaluated numerically.

APPENDIX B: CROSSOVER EQUATION OF STATE OF KISELEV AND SENGERS

An alternative crossover equation of state has been proposed by Kiselev and Sengers and applied to represent the thermodynamic properties of methane and ethane in a large range of temperatures and densities around the critical point [35]. This alternative crossover equation of state is expressed in terms of parametric variables r and θ that are defined by the transformation

$$\tau = r(1 - b^2\theta^2) \tag{B1}$$

$$\Delta\tilde{p} - d_1\tau = kr^\beta\theta R^{-\beta+1/2}(rg) \tag{B2}$$

with

$$R(q) = 1 + \frac{q^2}{q_0 + q} \tag{B3}$$

Here $b^2 = (\gamma - 2\beta)/\gamma(1 - 2\beta)$ and $q_0 = 0.3$ are universal constants, where $\gamma = (2 - \eta)\nu$ and $\beta = (3\nu - \gamma)/2$, while g is a system-dependent constant that is inversely proportional to the so-called Ginzburg number [13, 65]. In terms of these variables the crossover equation for the reduced Helmholtz free-energy density has the form

$$\Delta\tilde{A}(r, \theta) = kr^{2-\alpha}R^\alpha(rg) \left[a\Psi_0(\theta) + \sum_{i=1}^5 c_i r^{\Delta_i} R^{-\tilde{\Delta}_i}(rg) \Psi_i(\theta) \right] \tag{B4}$$

where $\Psi_i(\theta)$ are universal functions of the parameter θ presented in Table III in the article by Kiselev and Sengers [35]. However, in that article the exponents $\tilde{\Delta}_i$ of the factor $R^{-\tilde{\Delta}_i}(rg)$ in Eq. (B4) were incorrectly identified with the exponents Δ_i of the factor r^{Δ_i} for $i \geq 3$. Equation (B4) replaces Eq. (39) and (A1) in Ref. 35, and Eqs. (A10)–(A13) in Ref. 35 should read

$$\tilde{\Delta}_1 = \Delta_1 = \nu\omega \tag{B5}$$

$$\tilde{\Delta}_2 = \Delta_2 = 2\Delta_1 \tag{B6}$$

$$\Delta_3 = \Delta_4 = \gamma + \beta - 1, \quad \tilde{\Delta}_3 = \tilde{\Delta}_4 = \Delta_3 - 1/2 \tag{B7}$$

$$\Delta_5 = \nu\omega_5, \quad \tilde{\Delta}_5 = \Delta_5 - 1/2 \tag{B8}$$

We also note that Fig. 8 in Ref. 35 does not show the isobaric specific-heat capacity C_p of methane but of ethane, as correctly stated in the caption of this figure.

The equation of Kiselev and Sengers represents a more phenomenological approach to deal with the crossover problem. However, being expressed in parametric variables r and θ directly, the equation is simpler for computer programming, since it avoids the iteration associated with obtaining the solution of the coupled equations (18) and (19) as discussed by Luettmmer-Strathmann et al. [20]. The crossover equation of state of Kiselev and Sengers, applied to methane and ethane, is valid in a range of temperatures and densities comparable to that of the crossover equation of state formulated in the present paper. Hence, an alternative practical crossover equation of state for mixtures of methane and ethane may be obtained by making the system-dependent coefficients in the equation of Kiselev and Sengers ζ dependent as was done by Povodyrev et al. [51] for the asymptotic critical behavior of the thermodynamic properties of methane and ethane.

ACKNOWLEDGMENTS

The authors are indebted to M. A. Anisimov and H. R. van den Berg for many valuable discussions. The research at the University of Maryland was supported by the Division of Chemical Sciences of the Office of Basic Energy Sciences of the U.S. Department of Energy under Grant DE-FG02-95ER-14509.

REFERENCES

1. M. E. Fisher, in *Critical Phenomena, Vol. 186 of Lecture Notes in Physics*, J.W. Hahne, ed. (Springer-Verlag, Berlin, 1982), p. 1.
2. J. V. Sengers and J. M. H. Levelt Sengers, *Annu. Rev. Phys. Chem.* **37**:189 (1986).
3. M. A. Anisimov, *Critical Phenomena in Liquids and Liquid Crystals* (Gordon and Breach, Philadelphia, 1991).
4. R. B. Griffiths and J. C. Wheeler, *Phys. Rev. A* **2**:1047 (1970).
5. W. F. Saam, *Phys. Rev. A* **2**:1461 (1970).
6. M. A. Anisimov, A. V. Voronel, and E. E. Gorodetskii, *Sov. Phys. JETP* **33**:605 (1971).
7. Z. Y. Chen, A. Abbaci, S. Tang, and J. V. Sengers, *Phys. Rev. A* **42**:4470 (1990).
8. G. X. Jin, S. Tang, and J. V. Sengers, *Phys. Rev. E* **47**:388 (1993).
9. G. X. Jin, *Effects of Critical Fluctuations on the Thermodynamic Properties of Fluids and Fluid Mixtures*, Ph.D. thesis (Institute for Physical Science and Technology, University of Maryland, College Park, MD, 1993).
10. J. C. Rainwater, in *Supercritical Fluid Technology*, J. F. Ely and T. J. Bruno, eds. (CRC Press, Boca Raton FL, 1991), p. 57.
11. M. A. Anisimov and J. V. Sengers, *Phys. Lett. A* **172**:114 (1992).
12. S. Tang and J. V. Sengers, *J. Supercrit. Fluids* **4**:209 (1991).
13. M. A. Anisimov, S. B. Kiselev, J. V. Sengers, and S. Tang, *Physica A* **188**:487 (1992).
14. J. V. Sengers, in *Supercritical Fluids*, E. Kiran and J. M. H. Levelt Sengers, eds. (Kluwer, Dordrecht, 1994), p. 231.
15. S. S. Leung and R. B. Griffiths, *Phys. Rev. A* **8**:2673 (1973).

16. A. J. Liu and M. E. Fisher, *Physica A* **156**:35 (1989).
17. F. C. Zhang and R. K. P. Zia, *J. Phys. A* **15**:3303 (1982).
18. G. X. Jin, J. V. Sengers, and S. Tang, to be published.
19. Z. Y. Chen, P. C. Albright, and J. V. Sengers, *Phys. Rev. A* **41**:3161 (1990).
20. J. Luettmer-Strathmann, S. Tang, and J. V. Sengers, *J. Chem. Phys.* **97**:2705 (1992).
21. S. Tang, J. V. Sengers, and Z. Y. Chen, *Physica A* **179**:344 (1991).
22. J. F. Nicoll and J. K. Bhattacharjee, *Phys. Rev. B* **23**:389 (1981).
23. D. G. Friend and F. Ely, *Fluid Phase Equil.* **79**:77 (1992).
24. D. G. Friend, *NIST Mixture Property Program*, NIST14, Version 9.08 (National Institute of Standards and Technology, Gaithersburg, MD, 1992).
25. D. G. Friend and M. L. Huber, *Int. J. Thermophys.* **15**:1279 (1994).
26. G. X. Jin, S. Tang, and J. V. Sengers, *Int. J. Thermophys.* **13**:671 (1992).
27. U. Setzmann and W. Wagner, *J. Chem. Ref. Data* **20**:1 (1991).
28. R. Kleinrahm and W. Wagner, *J. Chem. Thermodynam.* **18**:739 (1986).
29. R. Kleinrahm, W. Duschek, and W. Wagner, *J. Chem. Thermodynam.* **18**:1103 (1986).
30. G. Handel, R. Kleinrahm, and W. Wagner, *J. Chem. Thermodynam.* **24**:685 (1992).
31. N. G. Trappeniers, T. Wassenaar, and J. C. Abels, *Physica A* **98**:289 (1979); **100**:660 (1980).
32. B. A. Younglove, *J. Res. Natl. Bur. Stand. (USA)* **78A**:401 (1974).
33. H. M. Roder, *J. Res. Natl. Bur. Stand. (USA)* **80A**:739 (1976).
34. M. A. Anisimov, V. G. Beketov, V. P. Voronov, V. B. Nagaev, and V. A. Smirnov, *Teplofiz. Svoistva Veshchestv Mater. (USSR)* **16**:124 (1982).
35. S. B. Kiselev and J. V. Sengers, *Int. J. Thermophys.* **14**:1 (1993).
36. B. E. Gammon and D. R. Douslin, *J. Chem. Phys.* **64**:203 (1976).
37. G. C. Straty, *Cryogenics* **14**:367 (1974).
38. J. P. M. Trusler and M. Zazari, *J. Chem. Thermodynam.* **29**:973 (1992).
39. P. H. G. Kasteren and H. Zeldenrust, *Ind. Eng. Chem. Fundam.* **18**:333 (1979).
40. M. L. Jones, D. T. Mage, R. C. Faulkner, and D. L. Katz, *Chem. Eng. Proc. Symp. Ser.* **59**:52 (1963).
41. D. R. Douslin and R. H. Harrison, *J. Chem. Thermodynam.* **5**:491 (1973).
42. N. G. Shmakov, *Teplofiz. Svoistva Veshchestv. Materialov (Thermophysical Properties of Substances and Materials, Gosstandard, Moscow)* **7**:155 (1973).
43. D. Balzarini and M. Burton, *Can. J. Phys.* **57**:1516 (1979).
44. M. R. Moldover and J. S. Gallagher, *AIChE J.* **24**:268 (1978).
45. S. B. Kiselev, *High Temp.* **26**:337 (1988).
46. M. A. Anisimov, S. B. Kiselev, and I. G. Kostukova, *J. Heat Transfer Trans. ASME* **110**:986 (1988).
47. J. C. Rainwater, *Vapor-Liquid Equilibrium of Binary Mixtures in the Extended Critical Region. I. Thermodynamic Model*, NIST Technical Note 1328 (U.S. Government Printing Office, Washington, DC, 1989).
48. M. A. Anisimov and S. B. Kiselev, *Sov. Phys. Rev. Ser. B Therm. Phys.* **3**(2):1 (1992).
49. G. X. Jin, S. Tang, and J. V. Sengers, *Fluid Phase Equil.* **75**:1 (1992).
50. S. B. Kiselev and A. A. Povodyrev, *Fluid Phase Equil.* **79**:33 (1992).
51. A. A. Povodyrev, S. B. Kiselev, and M. A. Anisimov, *Int. J. Thermophys.* **14**:1187 (1993).
52. J. C. Rainwater and D. G. Friend, *Phys. Lett. A* **191**:431 (1994).
53. W. H. Haynes, R. D. McCarty, and B. E. Eaton, *J. Chem. Thermodynam.* **17**:209 (1985).
54. M. D. Bespalov, V. B. Nagaev, V. A. Smirnov, and S.-E. Khalidov, *Teplofiz. Svoistva Veshchestv Mater. (USSR)* **27**:32 (1989).
55. V. B. Nagaev, V. A. Smirnov, and S.-E. Khalidov, *Teplofiz. Svoistva Veshchestv Mater. (USSR)* **27**:20 (1989).

56. J. E. Mayrath and J. W. Magee, *J. Chem. Thermodynam.* **21**:499 (1989).
57. R. T. Ellington, B. E. Eakin, J. D. Parent, D. C. Gami, and O. T. Blommer, in *Thermodynamic and Transport Properties of Gases, Liquids and Solids*, Y. S. Touloukian, ed. (McGraw-Hill, New York, 1959), p. 180.
58. S. B. Kiselev, S.-E. Khalidov, and A. V. Yudin, *J. Eng. Phys.* **54**:543 (1988).
59. O. T. Bloomer, D. C. Gami, and J. D. Parent, *Physical-Chemical Properties of Methane-Ethane Mixtures*, Institute of Gas Technology Research Bulletin **22** (1953).
60. V. Wichterle and R. Kobayashi, *J. Chem. Eng. Data* **17**(1):9 (1972).
61. J. Davalos, W. R. Anderson, R. E. Phelps, and A. J. Kidney, *J. Chem. Eng. Data* **21**(1):81 (1976).
62. B. A. Younglove, N. V. Frederick, and R. D. McCarty, *Speed of Sound Data and Related Models for Mixtures of Natural Gas Constituents*, NIST Technical Note 178 (U.S. Government Printing Office, Washington, DC, 1993).
63. A. Anisimov, E. E. Gorodetskii, V. D. Kulikov, and J. V. Sengers, *Phys. Rev. E* **51**:1199 (1995).
64. M. A. Anisimov, E. E. Gorodetskii, V. D. Kulikov, A. A. Povodyrev, and J. V. Sengers, *Physica A* **220**:277 (1995); **223**:272 (1996).
65. S. B. Kiselev, *High Temp.* **28**:42 (1990).